Supplementary Material of
Free-electron-driven X-ray caustics
from strained van der Waals materials

Contents

Section 1 | The scattering field of a free electron by a 2D crystal layer

When a free electron traverses a 2D crystal layer with Bravais lattice spanning the x-y plane at z=0, the electromagnetic field that accompanies the free electron is scattered by a collection of atoms modeled as a dipole array characterized by their linear atomic polarizability. To exploit the discrete translational symmetry of the lattice, we use the 2D Fourier transform[1] of a function $f(\mathbf{R})$ located at the lattice sites $\mathbf{r}_n$=($\mathbf{R}_n$, 0), f_n=$f(\mathbf{r}_n)$, defined as

$$f(\mathbf{Q}) = A\sum_{n=1}^{\infty} e^{-i\mathbf{Q}\cdot\mathbf{R}_n} f_n, \tag{1}$$

$$f_n = \int_{\mathrm{BZ}} \frac{d^2\mathbf{Q}}{(2\pi)^2} e^{i\mathbf{Q}\cdot\mathbf{R}_\mathrm{n}} f(\mathbf{Q}),$$

where A is the area of the lattice unit cell and BZ indicates that the integral over $\mathbf{Q}$ is performed within the first Brillouin zone (BZ) of the reciprocal lattice.

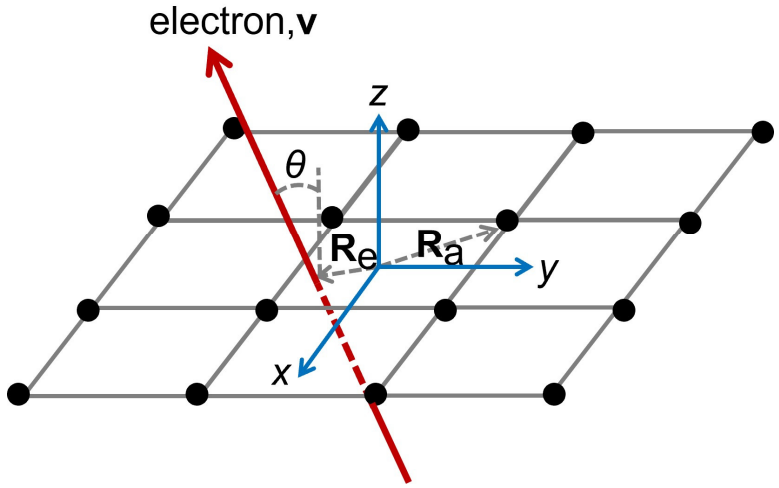

Figure s1 | Schematic of a free electron traversing a 2D crystal layer spanning the $x-y$ plane at z=0. The electron velocity forms an incidence angle θ with respect to the crystal layer normal. $\mathbf{R}_\mathrm{a}$ and $\mathbf{R}_\mathrm{e}$ denote the in-plane distances from the center of the unit cell to the atom and electron crossing position, respectively.

The free electron is described as a classical point charge in $\mathbf{r}$-t space, introducing its current density $\mathbf{J}(\mathbf{r},t) = -e\mathbf{v}\delta(\mathbf{r}-\mathbf{r}_\mathrm{e}-\mathbf{v}t)$, where $\mathbf{r}_\mathrm{e}$=$(\mathbf{R}_\mathrm{e},0)$ denotes the displacement of the electron in the z=0 plane at time t=0, and $\mathbf{v}$ is the electron velocity vector. The current density in $\mathbf{q}$-ω space is $\mathbf{J}(\mathbf{q},\omega) = -2\pi e\mathbf{v}e^{-i\mathbf{q}\cdot\mathbf{R}_\mathrm{e}}\delta(\omega-\mathbf{q}\cdot\mathbf{v})$. The electromagnetic field that accompanies the free electron is then[2]

$$\begin{aligned}\mathbf{E}^{\mathrm{inc}}(\mathbf{r},\omega) &= 2i\pi\omega\mu_0 e\int\frac{d^3\mathbf{q}}{(2\pi)^3}\left(\bar{\bar{\mathrm{I}}}-\frac{\mathbf{qq}}{k^2}\right)\frac{e^{i\mathbf{q}\cdot(\mathbf{r}-\mathbf{r}_\mathrm{e})}}{k^2-q^2}\cdot\mathbf{v}\delta(\omega-\mathbf{q}\cdot\mathbf{v})\\ &= \frac{ie}{\varepsilon_0 v_z}\int\frac{d^2\mathbf{Q}}{(2\pi)^2}\frac{k\,\mathbf{v}/c-\mathbf{q}}{k^2-q^2}e^{i\mathbf{q}\cdot(\mathbf{r}-\mathbf{r}_\mathrm{e})} \qquad (2)\\ &= \int\frac{d^2\mathbf{Q}}{(2\pi)^2}\mathbf{E}^{\mathrm{inc}}(\mathbf{Q},\omega)e^{i\mathbf{Q}\cdot\mathbf{R}},\end{aligned}$$

where ω and $k=\omega/c$ are the photon angular frequency and wavenumber, μ_0 and ε_0 are the vacuum permeability and permittivity, $-e$ is the electron charge, $\mathbf{Q}$ is the x-y component of the

Fourier wave vector $\mathbf{q} = \left(\mathbf{Q}, \frac{\omega - \mathbf{Q}\cdot\mathbf{v}_\parallel}{v_z}\right)$ (notice that the z component is determined by the δ function in Eq. (2)), $\mathbf{R}$ is the x-y component of the position vector, $\mathbf{r}_\mathrm{e}$ is the position of the electron at time $t = 0$, and $\mathbf{E}^\mathrm{inc}(\mathbf{Q}, \omega)$ is the 2D Fourier transform of $\mathbf{E}^\mathrm{inc}(\mathbf{r}, \omega)$.

The atomic dipole moment at position $\mathbf{r}_\mathrm{d} = (\mathbf{R}_n + \mathbf{R}_\mathrm{a}, 0)$ is denoted as $\mathbf{p}_n = \alpha(\omega)\mathbf{E}^\mathrm{inc}(\mathbf{r}_\mathrm{d}, \omega)$, where $\mathbf{R}_n$ is the 2D lattice site position, $\mathbf{R}_\mathrm{a}$ is the position of the atom relative to the center of the unit cell, and $\alpha(\omega)$ is the atomic polarizability that can be derived from the scattering factor[3]. The field scattered by the 2D dipole array is

$$\mathbf{E}^\mathrm{sca}(\mathbf{r}, \omega) = \omega^2\mu_0 \sum_n \overline{\overline{\mathrm{G}}}(\mathbf{r} - \mathbf{r}_\mathrm{d}) \cdot \mathbf{p}_n(\omega), \tag{3}$$

where $\overline{\overline{\mathrm{G}}}(\mathbf{r} - \mathbf{r}_\mathrm{d})$ is the electromagnetic dyadic Green function. The latter can be expanded as $\overline{\overline{\mathrm{G}}}(\mathbf{r} - \mathbf{r}_\mathrm{d}) = \frac{i}{2k^2}\int \frac{d^2\mathbf{Q}}{(2\pi)^2}\frac{k^2 - \mathbf{kk}}{k_z} e^{i\mathbf{Q}\cdot(\mathbf{R}-\mathbf{R}_n-\mathbf{R}_\mathrm{a})+ik_z|z|}$, where $\mathbf{k} = (\mathbf{Q}, \pm k_z)$ and $k_z = \sqrt{k^2 - Q^2}$. The atomic dipole moment $\mathbf{p}_n(\omega)$ is also Fourier expanded following Eq. (1) as $\mathbf{p}_n(\omega) = \int_\mathrm{BZ} \frac{d^2\mathbf{Q}}{(2\pi)^2} e^{i\mathbf{Q}\cdot\mathbf{R}_n}\mathbf{p}(\mathbf{Q}, \omega)$. By making use of the identity $\sum_n e^{i\mathbf{Q}\cdot\mathbf{R}_n} = \sum_\mathbf{G} \frac{(2\pi)^2}{A}\delta(\mathbf{Q} - \mathbf{G})$, where $\mathbf{G}$ is the 2D reciprocal lattice vector and A is the area to a 2D unit cell, the electron scattering field in Eq. (3) becomes

$$\mathbf{E}^\mathrm{sca}(\mathbf{r}, \omega) = \frac{i}{2A\varepsilon_0}\int \frac{d^2\mathbf{Q}}{(2\pi)^2}\frac{k^2 - \mathbf{kk}}{k_z} \cdot \mathbf{p}(\mathbf{Q}, \omega) e^{i\mathbf{Q}\cdot(\mathbf{R}-\mathbf{R}_\mathrm{a})+ik_z|z|}. \tag{4}$$

It should be noted that $\mathbf{Q}$ is not limited to the first BZ and is periodic in reciprocal lattice space, and the idensity $\mathbf{p}(\mathbf{Q}, \omega) = \mathbf{p}(\mathbf{Q} + \mathbf{G}, \omega)$ follows from the definition in Eq. (1). Under the assumption of isotropic polarizabilities, the dipole moment $\mathbf{p}_n(\omega)$ is linearly polarized along the direction of the electron electric field at position $\mathbf{r}$=$(\mathbf{R}_n, 0)$. We also note that the linear polarizability is $\alpha(\omega)/(\varepsilon_0 V_\mathrm{cell}) \ll 1$ (of the same order as the susceptibility) in the X-ray range, where V_cell is the volume of one unit cell (i.e., the 2D unit cell area A times the interlayer spacing). The dipole-dipole interaction is neglected as it is of order $O(\alpha^2)$, and therefore, we have

$$\mathbf{p}_n(\omega) = \alpha(\omega)\mathbf{E}^\mathrm{inc}(\mathbf{r}_\mathrm{d}, \omega), \tag{5}$$

$$\mathbf{p}(\mathbf{Q},\omega) = \alpha(\omega)\sum_{\mathbf{G}} \mathbf{E}^{\mathrm{inc}}(\mathbf{Q}+\mathbf{G}\,,\omega)\, e^{i(\mathbf{Q}+\mathbf{G})\cdot\mathbf{R}_{\mathrm{a}}},$$

Where the latter equation is the Fourier transform of the former one, and $\mathbf{E}^{\mathrm{inc}}(\mathbf{Q}+\mathbf{G}\,,\omega)$ is the 2D Fourier transform of $\mathbf{E}^{\mathrm{inc}}(\mathbf{r},\omega)$ defined in Eq. (2). Combining Eqs. (2), (4), and (5), we have

$$\begin{aligned}\mathbf{E}^{\mathrm{sca}}(\mathbf{r},\omega) &= \frac{i\alpha(\omega)}{2A\varepsilon_0}\sum_{\mathbf{G}}\int \frac{d^2\mathbf{Q}}{(2\pi)^2}\frac{k^2-\mathbf{kk}}{k_z}\cdot\mathbf{E}^{\mathrm{inc}}(\mathbf{Q}+\mathbf{G}\,,\omega)e^{i\mathbf{Q}\cdot\mathbf{R}+i\mathbf{G}\cdot\mathbf{R}_{\mathrm{a}}+ik_z|z|}\\ &= -\frac{\alpha(\omega)e}{2Av_z\varepsilon_0^2}\sum_{\mathbf{G}}\int \frac{d^2\mathbf{Q}}{(2\pi)^2}\frac{k^2-\mathbf{kk}}{k_z}\\ &\qquad\cdot\frac{k\,\mathbf{v}/c-\mathbf{Q}_{\mathbf{G}}-q_z\hat{z}}{k^2-\mathbf{Q}_{\mathbf{G}}^2-q_z^2}e^{i\mathbf{G}\cdot(\mathbf{R}_{\mathrm{a}}-\mathbf{R}_{\mathrm{e}})+i\mathbf{Q}\cdot(\mathbf{R}-\mathbf{R}_{\mathrm{e}})+ik_z|z|},\end{aligned} \tag{6}$$

where $k_z=\sqrt{k^2-Q^2}$, $\mathbf{Q}_{\mathbf{G}}=\mathbf{Q}+\mathbf{G}$ and $q_z=\frac{\omega-\mathbf{Q}_{\mathbf{G}}\cdot\mathbf{v}}{v_z}$. Using the saddle-point approach and the Weyl identity $\frac{e^{ikr}}{r}=\frac{i}{2\pi}\int d^2\mathbf{Q}\frac{e^{i(k_xx+k_yy+k_z|z|)}}{k_z}$, we arrive at the following analytical expression for the scattering field produced by a free electron upon interaction with the atomic array:

$$\mathbf{E}^{\mathrm{sca}}(\mathbf{G},\mathbf{r},\omega) = \frac{ie\alpha(\omega)}{Av_z\varepsilon_0^2}(k^2-\mathbf{kk})\cdot\frac{k\,\mathbf{v}/c-\mathbf{Q}_{\mathbf{G}}-q_z\hat{z}}{k^2-\mathbf{Q}_{\mathbf{G}}{}^2-q_z^2}\frac{e^{ikr'+i\mathbf{G}\cdot(\mathbf{R}_{\mathrm{a}}-\mathbf{R}_{\mathrm{e}})}}{4\pi r'}, \tag{7}$$

where $r'=|\mathbf{r}-\mathbf{r}_{\mathrm{e}}|$ is the far-field distance from the point where the electron transverses the 2D layer.

Section 2 | The dispersion of PXR emission from a bent crystal

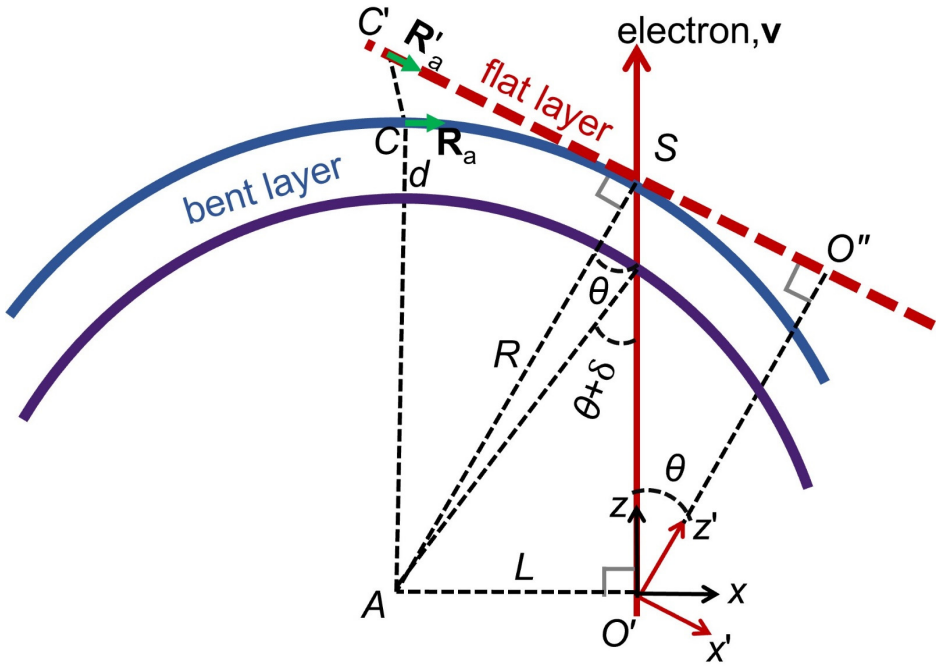

Figure s2 | Substituting flat layers for bent layers. The atomic positions along the line AC remain fixed during the bending process. A free electron (red arrow) traverses a bent layer (blue curve) at point S. The electron trajectory and the radial line AC are parallel and separated by a distance L. The blue bent layer is substituted by a flat layer (dashed red line) with the tangential point S. We introduce two frames: the x-z frame, in which the electron moves along the z-axis, and the x'-z' frame, in which the z' axis is perpendicular to the flat layer located at $z'=R\cos^2\theta$. Here, R is the radius of the bent layer and θ is the electron incidence angle relative to the normal direction (shared by the flat layer and the curved one to which is substitutes).

We substitute the bent multilayers by a series of flat layers of different orientations relative to each other. Their positions and normal vectors are determined to match those of the bent vdW structure at the points where the electron crosses the corresponding bent layers. We sketch in Fig. s2 how a bent layer (blue curve) can be substituted by a flat layer (dashed red line). We can image the bent layer being flattened around the point S without shearing deformation, and thus, the atomic positions around point S are the same in both layers. We consider that the crystal structure is cylindrically bent with mirror and translational symmetry along the radial line AC, so that the atom positions along such line remain invariant during the bending process. The point C on the bent layer is projected onto the point C' on the flat layer with the same in-plane distance to the tangential point S, such that $\overline{SC'} = \overset{\frown}{SC}$. From Eq. (7), we know that when the 2D Bravais lattice

sits in the $z = 0$ plane and the electron passes through the 2D lattice at the origin point, the phase of the scattered field is $\phi = kr + \mathbf{G} \cdot \mathbf{R}_\mathrm{a}$. However, when the free electron passes through the equivalent flat layer in Fig. s2, the phase equation should be modified to include the changes of the electron impacting position and the atomic position $\mathbf{R}_\mathrm{a}$.

Vectors and their components in the $x - y$ ($x' - y'$) frame are denoted without (with) prime. We repeat the scattered field calculation from Eqs. (1) to (6) in the $x'-z'$ frame with the 2D flat layer located at $z' = R\cos^2\theta$ and the electron passing by point O' at time $t = 0$. The phase factor in the equation is thus $e^{i\mathbf{G}'\cdot\mathbf{R}'_\mathrm{a}+i\mathbf{Q}'\cdot\mathbf{R}'+ik_z|z-R\cos^2\theta|+iq'_zR\cos^2\theta}$, where $q'_z = \left[\omega - (\mathbf{Q}' + \mathbf{G}')\cdot\mathbf{v}'_\parallel\right]/v'_z$, $\mathbf{v}'_\parallel$ and v'_z are the electron velocity components in the $x'-z'$ frame, $\mathbf{v} = -v\sin\theta\,\hat{x}' + v\cos\theta\,\hat{z}'$, and $\mathbf{R}'_\mathrm{a}$ is the atomic relative position in the $x' - y'$ frame.

We need to define $\mathbf{R}'_\mathrm{a}$ in a way such that it maintains the match of the atomic positions between the bent layer and the flat layer around the tangent point S. The in-plane atomic position of the bent layer $\mathbf{R}_\mathrm{a} = \sigma_1\hat{x} + \sigma_2\hat{y}$ relative to the line AC is marked by the green arrow. Correspondingly, $\mathbf{R}'_\mathrm{a}$ in the flat layer is defined relative to the point C' with $|\mathbf{R}_\mathrm{a}| = |\mathbf{R}'_\mathrm{a}|$ under the condition of plastic bending. In the $x' - z'$ frame, $\mathbf{R}'_\mathrm{a} = \sigma_1\hat{x}' + \sigma_2\hat{y}' - C'O'\hat{x}' = \sigma_1\hat{x}' + \sigma_2\hat{y}' - (R\theta + R\cos\theta\sin\theta)\hat{x}'$ with the 2D origin point at O''.

Consequently, the phase of the waves in the $x' - y'$ frame becomes $e^{i\mathbf{G}'\cdot(\sigma_1\hat{x}'+\sigma_2\hat{y}')-iG'_xR\theta+i\mathbf{Q}'\cdot(\mathbf{R}'+R\cos\theta\sin\theta\hat{x}')+ik_z|z'-R\cos^2\theta|+i\frac{\omega}{v}R\cos\theta}$. We use the saddle point approach to derive the far-field phase, that is, $\phi(\theta) = \mathbf{G}'\cdot(\sigma_1\hat{x}' + \sigma_2\hat{y}') - G'_xR\theta + \frac{\omega}{v}R\cos\theta + k|\mathbf{r} - R\cos\theta\,\hat{z}|$. It should be noted that we have $\mathbf{G}'\cdot(\sigma_1\hat{x}' + \sigma_2\hat{y}') = \mathbf{G}\cdot(\sigma_1\hat{x} + \sigma_2\hat{y})$ under the condition of plastic bending.

The relation between the incidence angle θ, its variation δ in the neighboring layer, and the interlayer distance d is $d = \frac{L}{\sin\theta} - \frac{L}{\sin(\theta+\delta)} \simeq L\frac{\cos\theta}{\sin^2\theta}\delta$. The radius is related to the incidence angle θ through $R\sin\theta = L$. The dispersion of radiation from the bent layers is obtained from $\phi(\theta + \delta) - \phi(\theta) = 2n\pi$, where n is an integer. This leads to

$$k\frac{z - L\cot\theta}{|\mathbf{r} - L\cot\theta\,\hat{z}|} = -\frac{2n\pi}{d}\cos\theta + \frac{\omega}{v} + G'_x(\sin\theta - \theta\cos\theta), \qquad (8)$$

which is Eq. (2) in the main text, with G_x' replaced by $g_{\parallel}$ and $\frac{2n\pi}{d}$ replaced by $g_{\perp}$.

Section 3 | The trajectory equation of the X-ray Airy beam

From ray optical theory, Eq. (8) shows the θ-dependent trajectory of the rays, as shown in Fig. 1b of the main text. The envelope equation of the rays can be obtained by combining Eq. (8) and its derivative, that is,

$$\begin{aligned} k\frac{z-L\cot\theta}{|\mathbf{r}-L\cot\theta\,\hat{z}|} &= -\frac{2n\pi}{d}\cos\theta+\frac{\omega}{v}+G_x'(\sin\theta-\theta\cos\theta), \\ k\frac{\partial}{\partial\theta}\frac{z-L\cot\theta}{|\mathbf{r}-L\cot\theta\,\hat{z}|} &= \frac{\partial}{\partial\theta}\left[-\frac{2n\pi}{d}\cos\theta+\frac{\omega}{v}+G_x'(\sin\theta-\theta\cos\theta)\right]. \end{aligned} \tag{9}$$

Indeed, combing these two equations, we obtain the envelope equation

$$|\mathbf{r}-L\cot\theta\,\hat{z}| = \frac{L}{-\frac{2n\pi c}{d\omega}\sin^3\theta}\left[1-\left(\frac{2n\pi c}{\omega d}\cos\theta+\frac{c}{v}\right)^2\right], \tag{10}$$

where we set $G_x'=0$ because our numerical results show that this component dominates over the contribution of all other in-plane reciprocal lattice vectors.

The radius of the central layer is R, as indicated in Fig. s2. We also consider here another layer with radius $R+t$. The respective electron incidence angles are θ_0 and $\theta_0+\delta\theta$, with $\sin\theta_0 = L/R$ and $L\frac{\cos\theta_0}{\sin^2\theta_0}\delta\theta \cong t$ under the condition $t \ll R$. Performing a Taylor expansion on both sides of Eq. (10), we have

$$
\begin{aligned}
&|\mathbf{r} - L\cot\theta\,\hat{z}\,| = \\
&\quad -\frac{L}{\frac{2n\pi c}{d\omega}}\frac{1}{\sin^3\theta_0}\left[1-\left(\frac{2n\pi c}{d\omega}\cos\theta_0+\frac{c}{v}\right)^2\right] \\
&\qquad +\frac{L}{-\frac{2n\pi c}{d\omega}}\frac{1}{\sin^2\theta_0}\left[\frac{4c^2n\pi(d\omega+2n\pi v\cos\theta_0)}{d^2\omega^2 v}\right. \\
&\qquad \left. -3\left(1-\left(\frac{c}{v}+\frac{2n\pi c\cos\theta_0}{d\omega}\right)^2\right)\frac{\cos\theta_0}{\sin^2\theta_0}\right]\delta\theta \\
&\qquad -L\left(\frac{2n\pi c}{d\omega}\cos\theta_0+\frac{c}{v}\right)\frac{\delta\theta}{\sin^2\theta_0} \\
&= -\frac{L}{\frac{2n\pi c}{d\omega}}\frac{1}{\sin^3\theta_0}\left[1-\left(\frac{2n\pi c}{d\omega}\cos\theta_0+\frac{c}{v}\right)^2\right] \\
&\qquad +\frac{1}{-\frac{2n\pi c}{d\omega}}\left[\frac{4c^2n\pi(d\omega+2n\pi v\cos\theta_0)}{d^2\omega^2 v\cos\theta_0}\right. \\
&\qquad \left. -3\left(1-\left(\frac{c}{v}+\frac{2n\pi c\cos\theta_0}{d\omega}\right)^2\right)\frac{1}{\sin^2\theta_0}\right]t \\
&\qquad -\left(\frac{2n\pi c}{d\omega}+\frac{c}{v\cos\theta_0}\right)t \\
&= -\frac{d\omega}{2n\pi c}\frac{R^3}{L^2}\sin^2\varphi_0+3\left(-\frac{\cos\varphi_0}{\cos\theta_0}+\frac{d\omega}{2n\pi c}\frac{\sin^2\varphi_0}{\sin^2\theta_0}\right)t
\end{aligned}
\tag{11}
$$

where $\cos\varphi_0=\frac{1}{\beta}+\frac{n\lambda}{d}\cos\theta_0$ and $\cos\theta_0=\sqrt{1-\left(\frac{L}{R}\right)^2}$. The first term following the last equality represents the focal distance of the Airy beam, while the second term stands for the caustic axial distribution.

Section 4 | Justifying the substitution of a bent layer by a flat layer

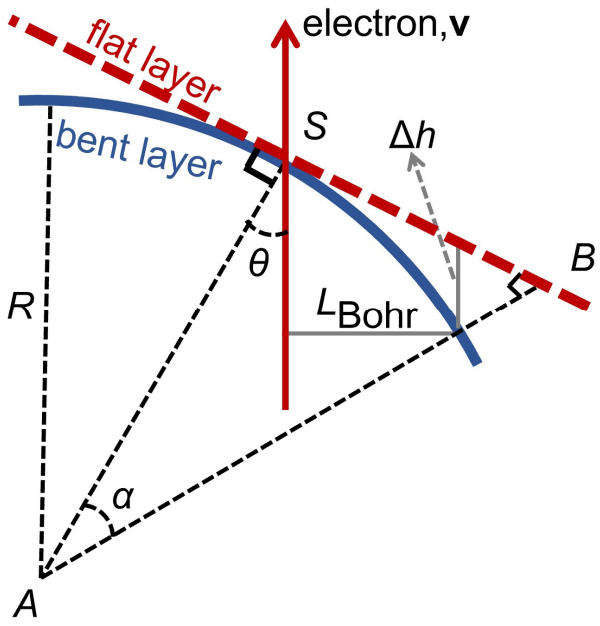

Figure s3 | Error produced by substituting a bent layer by a flat layer. The flat layer is tangential to the bent layer at point S, which is the electron impact point on the bent layer. The difference between the electron scattered fields in the two types of layers is estimated by discussing the phase difference of the dipoles on the two layers within the range of the electron Bohr cutoff ($L_{\mathrm{Bohr}}=v\gamma/\omega$), where v is the electron velocity, γ is the Lorentz contraction factor, and ω is the angular frequency.

We use a flat crystal layer to substitute the bent crystal layer in our calculation. In what follows, we justify the approximation by comparing the phase difference of the electron excited dipoles on the flat layer and the bent layer within the Bohr cutoff range $L_{\mathrm{Bohr}}=v\gamma/\omega$, where $\gamma=1/\sqrt{1-v^2/c^2}$ is the Lorentz contraction factor. We note that L_{Bohr} measures the distance up to which the free electron field takes significant values (i.e., its spatial extension away from the electron trajectory). The Bohr cutoffs for (1) a 300 keV electron and 3 keV photon energy, (2) a 1 MeV electron and 3 keV photon energy, and (3) a 10 MeV electron and 10 keV photon energy are (1) 0.08 nm, (2) 0.18 nm, and (3) 0.40 nm, respectively.

The phase variation of the field supplied by a free electron moving along the z direction is $\omega z/v$. Therefore, the phase difference of the electron excited dipoles on two consecutive layers along the electron trajectory at the Bohr cutoff is $\frac{\omega}{v}\Delta h$, as shown in Fig. s3. We have $\Delta h=\frac{AB-R}{\cos\theta}$

by applying the approximation that OB is parallel to OA under the condition that $L_{\mathrm{Bohr}} \ll R$, since $AB - R = \frac{R}{\cos\alpha} - R = \frac{\alpha^2}{2}R$, $\Delta h = \frac{1}{2}\left(\frac{\frac{L_{\mathrm{Bohr}}}{\cos\theta}}{R}\right)^2 \frac{R}{\cos\theta} = \frac{1}{2}\frac{L_{\mathrm{Bohr}}^2}{R\cos^3\theta}$. The phase difference is thus $\frac{\omega}{v}\Delta h = \frac{\beta\gamma^2\lambda}{4\pi R\cos^3\theta}$, where $\beta = \frac{v}{c}$. When the phase difference satisfies $\frac{\omega}{v}\Delta h \ll \frac{\pi}{2}$, the substitution is justifiable. In the main text, the kinetic energy of the electron is set to 1 MeV, the photon energy is 3 keV, the bending radius is $R = 5$ μm, and the incidence angle is $\theta \simeq \sin^{-1}\left(\frac{4}{5}\right)$, and therefore, we have $\frac{\omega}{v}\Delta h \simeq 10^{-4} \ll 1$.

Section 5 | X-ray Airy beam from elastically bent vdW materials

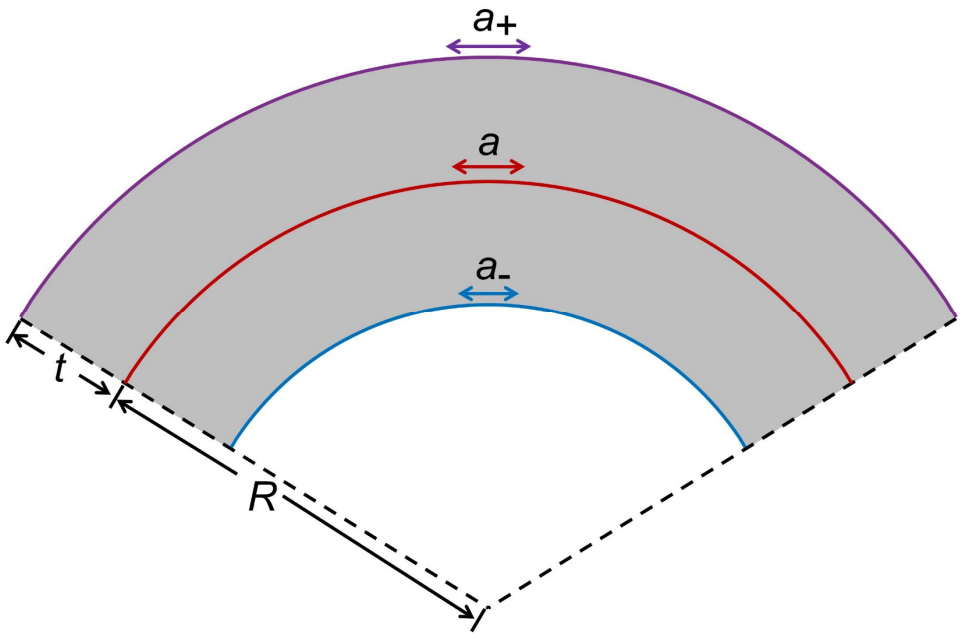

Figure s4 | Lattice variation of an elastic bending multilayer structure (cross section). The red curve represents the length-invariant surface. The double arrows represent the in-plane lattice constants, which are directly proportional to the radii.

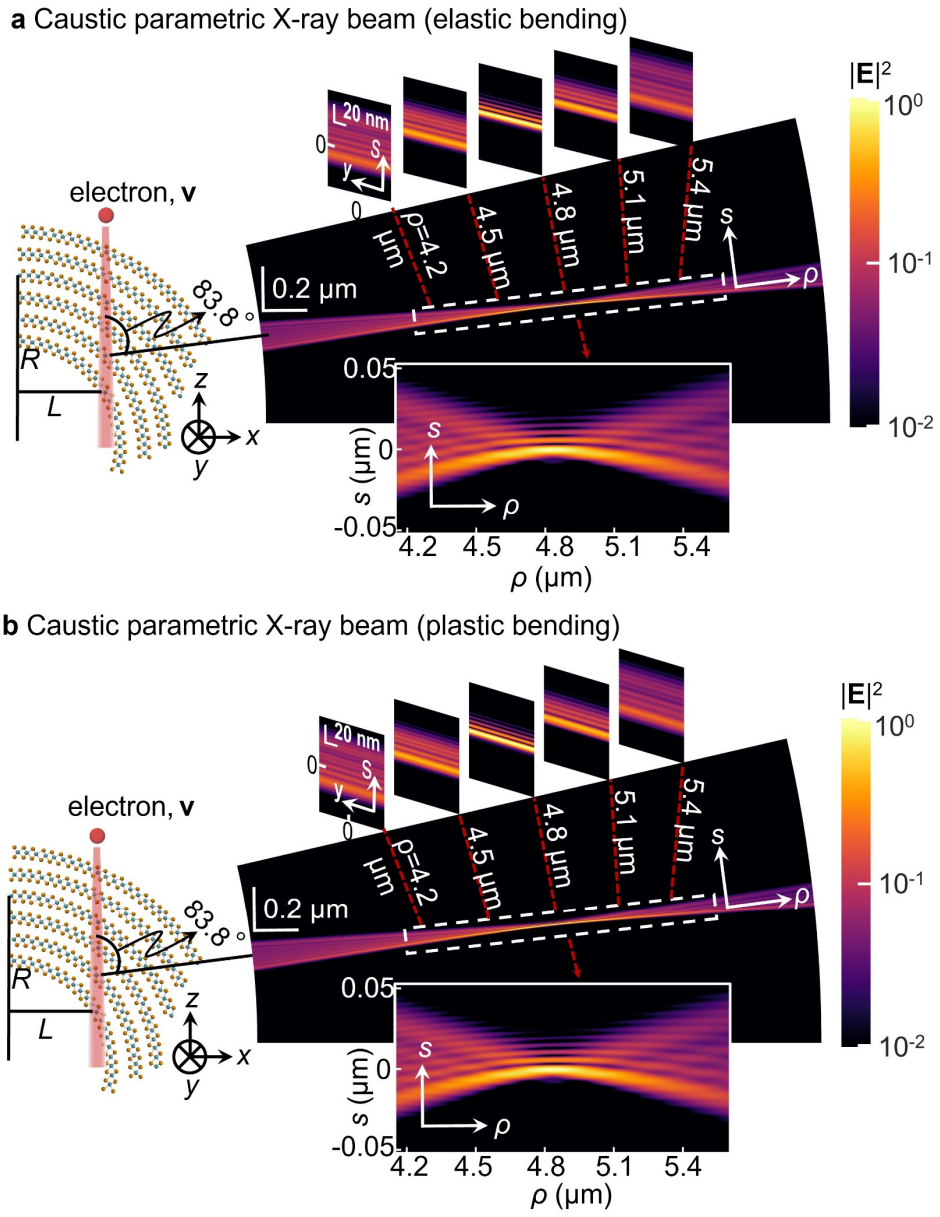

Figure s5 | Caustic X-ray beam from a cylindrically bent multilayer WSe_2 heterostructure modelled in the (a) elastic bending and (b) plastic bending configurations. In the elastic bending model, the in-plane lattice constants are extended or compressed during the bending process, so the in-plane reciprocal lattices are correspondingly scaled down or up. In the plastic bending model, the in-plane lattice constants and reciprocal lattices remain invariant. The numerical results in both configurations are nearly identical because the caustic beam is mainly contributed by a zero in-plane reciprocal lattice vector.

If the multilayers are perfectly glued together, they bend as a single plate following the continuum mechanics plate theory. We consider a cylindrically bent plate with the cross section shown in Fig. s4. The red curve is the length-invariant neutral surface, away from which the layers are extended (e.g., the purple curved surface) or compressed (e.g., the blue curved surface) parallel to it by

scales that are proportional to the distances from the neutral surface, and therefore, the magnitudes of in-plane reciprocal lattice vectors are inversely proportional to the radii. In Fig. s5, we compare the X-ray Airy beam generated from a bent WSe_2 multilayer structure modelled as elastic bending (Fig. s5a) or plastic bending (Fig. s5b). The numerical results show that there is no significant difference between the two results, as the specific Airy beam plotted in the image is mainly contributed by the zero reciprocal lattice vector.

Section 6 | Photon density operator

The reduced density operator of the photons is $\rho_{\mathrm{ph}} = \mathrm{Tr}_{\mathrm{ele}}(|f\rangle\langle f|)$, which is constructed from the final states of the joint system $|f\rangle = \sum_{\mathbf{p}',\mathbf{k}} \frac{1}{\sqrt{V}} \psi(\mathbf{k},\mathbf{p}')|\mathbf{p}'\rangle \otimes |1_{\mathbf{k}}\rangle$. We can also write ρ_{ph} as

$$\rho_{\mathrm{ph}} = \frac{1}{V} \sum_{\mathbf{p}'} \sum_{\mathbf{k},\mathbf{k}'} \psi(\mathbf{k},\mathbf{p}')\psi^*(\mathbf{k}',\mathbf{p}')|1_{\mathbf{k}}\rangle\langle 1_{\mathbf{k}'}|. \tag{12}$$

Section 7 | Quantum aspects of the generation of X-ray caustics

For regular periodic crystals, the vector potential modes are written from Bloch's theorem as[4]

$$\mathbf{A}(\mathbf{r}) = \sum_{\{\mathrm{n}\},\mathbf{k}} \mathbf{A}_{\mathbf{g},\mathbf{k}} e^{i(\mathbf{k}+\mathbf{g})\cdot\mathbf{r}} + c.c. = \sum_{\{\mathrm{n}\},\mathbf{k}} \mathbf{u}_{\mathbf{g},\mathbf{k}} e^{i(\mathbf{k}+\mathbf{g})\cdot\mathbf{r}} a_{\mathbf{k}} + \mathrm{c.c.}, \tag{13}$$

where the {n} sum runs over the reciprocal lattices. The crystal structure of a bent vdW material is aperiodic because the crystal lattice rotates gradually along the electron trajectory, as shown in Fig. 1b of the main text. Therefore, the amplitude $\mathbf{u}_{\mathbf{g},\mathbf{k}}(\mathbf{r})$ and the reciprocal lattice vector $\mathbf{g}(\mathbf{r})$ are not constant but position dependent.

The initial electron-photon state is described as $|i\rangle = \sum_{\mathbf{p}} \frac{1}{\sqrt{V}} \psi(\mathbf{p})|\mathbf{p}\rangle \otimes |0\rangle$, where $\sum_{\mathbf{p}} \frac{1}{\sqrt{V}} \psi(\mathbf{p})|\mathbf{p}\rangle$ is the superposition of electron momentum states $|\mathbf{p}\rangle$ and $|0\rangle$ is the photon vacuum state. The final electron-photon state is $|f\rangle = \sum_{\mathbf{p}',\mathbf{k}} \frac{1}{\sqrt{V}} \psi(\mathbf{k},\mathbf{p}')|\mathbf{p}'\rangle \otimes |1_{\mathbf{k}}\rangle$. From Eq. (12), we

know that the interference of different photon states relies on the overlap of the spectral function $\psi(\mathbf{k}, \mathbf{p}')$. From the perturbation theory of quantum electrodynamics (QED),

$$\begin{aligned}&\psi(\mathbf{k}, \mathbf{p}')\\&= -\frac{i}{\hbar}\int_0^t dt_1 \sum_{\mathbf{p}} \psi(\mathbf{p}) \left\langle 1_{\mathbf{k}}, \mathbf{p}' \middle| e^{\frac{i}{\hbar}H_0^{(s)}t_1} \left\{-\frac{q}{m}\mathbf{P}\cdot\mathbf{A}(\mathbf{r})\right\} e^{-\frac{i}{\hbar}H_0^{(s)}t_1} \middle| 0, \mathbf{p} \right\rangle\end{aligned} \tag{14}$$

To evaluate the above equation, we proceed as follows:

$$\begin{aligned}&\left\langle 1_{\mathbf{k}}, \mathbf{p}' \middle| e^{\frac{i}{\hbar}H_0^{(s)}t_1} \left\{-\frac{q}{m}\mathbf{P}\cdot\mathbf{A}(\mathbf{r})\right\} e^{-\frac{i}{\hbar}H_0^{(s)}t_1} \middle| 0, \mathbf{p} \right\rangle\\&\qquad = \sum_{\{\mathrm{n}\}} \left\langle \mathbf{p}' \middle| -\frac{q}{m}\mathbf{P}\cdot\mathbf{u}_{\mathbf{g},\mathbf{k}} e^{i(\mathbf{k}+\mathbf{g})\cdot\mathbf{r}} \middle| \mathbf{p} \right\rangle e^{\frac{i}{\hbar}\left(-E_p+E_{p'}+\hbar\omega_k\right)t_1},\end{aligned}$$

where $E_{p'}$, E_p, and $\hbar\omega_k$ are the energies of the electron final state, the electron initial state, and the emitted photon, respectively. The evaluation of $\left\langle \mathbf{p}' \middle| -\frac{q}{m}\mathbf{P}\cdot\mathbf{u}_{\mathbf{g},\mathbf{k}} e^{i(\mathbf{k}+\mathbf{g})\cdot\mathbf{r}} \middle| \mathbf{p} \right\rangle$ cannot be carried out analytically because both $\mathbf{u}_{\mathbf{g},\mathbf{k}}$ and $\mathbf{g}$ are position dependent for aperiodic crystals. We denote it as the transition matrix element $\mathcal{M}_{kpp'}$. Then Eq. (16) becomes

$$\begin{aligned}&\psi(\mathbf{k}, \mathbf{p}')\\&= -\frac{i}{\hbar}\sum_{\mathbf{p},\{\mathrm{n}\}} \psi(\mathbf{p}) \left\langle \mathbf{p}' \middle| -\frac{q}{m}\mathbf{P}\cdot\mathbf{u}_{\mathbf{g},\mathbf{k}} e^{i(\mathbf{k}+\mathbf{g})\cdot\mathbf{r}} \middle| \mathbf{p} \right\rangle \int_0^t dt_1 e^{\frac{i}{\hbar}\left(-E_p+E_{p'}+\hbar\omega_k\right)t_1}\\&= -\frac{i}{\hbar}\sum_{\mathbf{p},\{\mathrm{n}\}} \psi(\mathbf{p}) \mathcal{M}_{kpp'}\, T\delta_{E_{p'}+\hbar\omega_k, E_p}\end{aligned} \tag{15}$$

where the energy conservation equation $T\delta_{E_{p'}+\hbar\omega_k,E_p} = \int_0^t e^{\frac{i}{\hbar}\left(-E_p+E_{p'}+\hbar\omega_k\right)t_1} dt_1$ is applied and T is the interaction time.

References

1. Shahmoon, E., Wild, D. S., Lukin, M. D. & Yelin, S. F. Cooperative Resonances in Light Scattering from Two-Dimensional Atomic Arrays. *Phys. Rev. Lett.* **118**, 113601 (2017).

2. García de Abajo, F. J. Optical excitations in electron microscopy. *Rev. Mod. Phys.* **82**, 209–275 (2010).

3. Chantler, C. T. Theoretical Form Factor, Attenuation, and Scattering Tabulation for Z=1–92 from E=1–10 eV to E=0.4–1.0 MeV. *J. Phys. Chem. Ref. Data* **24**, 71–643 (1995).

4. Nitta, H. Kinematical theory of parametric X-ray radiation. *Phys. Lett. A* **158**, 270–274 (1991).